Annuaire de l'Université de Sofia "St. Kliment Ohridski", Faculté de Physique, v. 112, 2020

MATERIAL CHARACTERIZATION IN THE MICROWAVE RANGE, WHEN THE NEW MATERIALS BECOME COMPOSITE, REINFORCED, 3D-PRINTED, ARTIFICIAL, NANOMATERIALS AND METAMATERIALS (Part 1)

PLAMEN I. DANKOV

Sofia University "St. Kliment Ohridski", Faculty of Physics, Department of Radio-Physics and Electronics, J. Bourchier blvd. 5, 1164-Sofia, Bulgaria

Пламен И. Данков, ХАРАКТЕРИЗИРАНЕ НА НОВИТЕ МАТЕРИАЛИ В МИКРОВЪЛНОВИЯ ДИАПАЗОН, КОГАТО ТЕ СТАВАТ ПОДСИЛЕНИ, КОМПОЗИТНИ, 3D-ПРИНТИРАНИ, ИЗКУСТВЕНИ, НАНО- И МЕТАМАТЕРИАЛИ (Част 1)

Разработването на разнообразни нови материали е ключов проблем на съвременния свят, приближаващ се към 5G комуникационното поколение и Индустрия 4.0. По тази причина, характеризирането на материалите (определяне на техните ключови параметри) играе важна роля. Диелектричните и магнитни константи и анизотропията на материалите могат да се измерват в микровълновия обхват; като интегрални характеристики те дават информация за образците като цяло и ние показваме как те могат да се свържат със състава на образците, тяхната структура, ориентацията на примесите, използваната технология, условията за създаване на образците и др. В тази първа част на работата ние представяме резюме на своите концепции, модели, измерителна методология и измерителни методи за екстракция на диелектричните и магнитни параметри на различни изкуствени материали, базирайки се на 18-годишен опит в областта на характеризиране на материалите в Микровълнова лаборатория във Физически факултет на Софийски Университет „Св. Климент Охридски".

Plamen I. Dankov, MATERIAL CHARACTERIZATION IN THE MICROWAVE RANGE, WHEN THE NEW MATERIALS BECOME COMPOSITE, REINFORCED, 3D-PRINTED, ARTIFICIAL, NANOMATERIALS AND METAMATERIALS (Part 2)

The development of new materials is a key issue of the modern world moving toward the 5G communication standard and Industry 4.0. Therefore, the characterization of these materials (determination of their key parameters) plays an important role. The dielectric and magnetic constants and material anisotropy can be measured in the microwave range; as integral characteristics, they give information for the whole sample and we have shown how they are bound with the sample composition, structure, inclusion orientation, technology, conditions for the sample growth and forming, etc. We present in this first part of the paper a summary of our concepts, models, measurement methodologies and measurement methods for extraction of the dielectric and magnetic parameters of different artificial materials, as results of our 18-year experience in the material characterization in the Microwave Laboratory of the Faculty of Physics in Sofia University, Bulgaria.

Keywords: 3D printed dielectrics, anisotropy, artificial dielectrics, ceramics, conductivity, metamaterials, microwave measurement methods, permeability, permittivity, textile fabrics

PACS numbers: 77.22.−d

For contact: Plamen Dankov, Sofia University "St. Kliment Ohridski", Faculty of Physics, 5, J. Bourchier blvd., 1164-Sofia, Bulgaria dankov@phys.uni-sofia.bg

1. INTRODUCTION

The new materials are a key issue of today's world. The mechanical and chemical engineers together with the physicists can construct now a variety of new artificial materials with quite specific properties, never met before in nature. As we mentioned in the title, the modern materials became reinforced, composite, 3D printed, mixed, nano-sized and meta-materials. First of all, these new materials will play a very important role for the realization of the current trends for automation and data exchange in manufacturing technologies within the modular structured smart factories or so-called fourth industrial revolution Industry 4.0. The second field of the modern materials' implementation is the forthcoming 5G communication standard, which will ensure the ability of machines, devices, sensors and people to connect and communicate with each other via the Internet of Things (IoT) or Internet of People (IoP). The third important area of application of the new materials is the sustainable development of human societies. All these future processes in the development of human civilization explain the needs to develop materials with a variety of new properties and the needs to have reliable ways to characterize these unique properties.

The characterization of materials usually means to specify their properties by different chemical, mechanical, optical, spectroscopic, electric, magnetic and other methods. The determination of the electromagnetic (EM) properties is also important when the new materials can be used in the modern electronics, wired and wireless communications, sensor networks, for specific electromagnetic wave propagation, electromagnetic compatibility, optical and microwave imaging, etc. The electromagnetic properties of materials are connected mainly with their complex dielectric and magnetic constants and related parameters as conductivity, refractive index, wavelength, propagation constants, phase/group velocities of waves, attenuations, penetration depths, cut-off and threshold conditions, etc. in the EM structures, where these materials have been incorporated. Due to these reasons, today many materials, known with some of their traditional applications can be considered as electrodynamic media, e.g. textile fabrics as antenna substrates, bio-tissues as electronic components, semiconductor structures as sensors for different macroscopic parameters of the environment, etc.

The laboratory for Microwave material characterization in the Faculty of Physics, Sofia University “St. Kliment Ohridski”, Bulgaria, has been orientated to determination mainly of the dielectric properties of the modern artificial materials: 3D printed dielectrics, reinforced substrates, ceramics, multi-layer antenna radomes, foams, absorbers, gradient dielectrics and magneto-dielectrics, textile fabrics, metamaterials, carbon-content materials, liquids, fresh plant tissues, etc. A special circumstance is the dielectric anisotropy of these materials (different permittivity along to different directions), which is very informative parameters and could be bound with the sample composition, structure, inclusions’ orientation, technology, conditions for sample growth and forming, etc.

In this review article, divided into two parts, we try to summarize the common issues of our 18-year research work for characterization of different materials in the whole microwave range, including the mm-wavelength range. A poster with the same title was presented on the interactive University poster exhibition of the Asia-Pacific Microwave Conference, Nov. 6-9, 2018, Kyoto, Japan [1].

First of all, we present here a classification of the modern materials from an electromagnetic point of view, their main electromagnetic parameters and how these parameters could be bounded with the structure, inclusions and used technology. Especially, we discuss the origins of the different types of artificial anisotropy with examples. Then we describe the developed in the laboratory variety of measurement methods for characterization of the material parameters in the microwave range (0.5-40 GHz), including several authorship methods. We include also in the part the proposed numerical models for reliable extraction of the material parameters from the obtained measurements results and discuss the basic principles and specific techniques for utilization of the commercial 3D electromagnetic simulators as auxiliary tools for extraction of the material parameters of the samples. In the second part of this paper [2], we illustrate our rich experience in the area of material characterization by presenting a lot of published and new concrete examples for determination of the parameters and specific properties of many commercial and unique artificial materials: the new generation of microwave substrates, ceramics and other crystal samples, multilayer radomes, foams, absorbers, gradient dielectrics and magneto-dielectrics, textile fabrics, 3D printed dielectrics, metamaterials, carbon-content materials, composites, liquids, fresh plant tissues, plasma, ferrites, etc. Finally, we unify the common issues of these examples and present some conclusions.

2. MAIN ELECTROMAGNETIC PARAMETERS OF MATERIALS IN THE MICROWAVE RANGE AND HOW THEY CAN BE USED FOR THEIR CHARACTERIZATION AND TECHNOLOGY CONTROL.

2.1. CLASSIFICATION OF MODERN MATERIALS

From the electrodynamic point of view, the materials could be characterized on the base of their response on the presence of electromagnetic fields in each considered electrodynamic system, where these materials have been incorporated. This response is determined by the properties of the materials, described by defining macroscopic scalar complex parameters: dielectric constant (permittivity) $\varepsilon = \varepsilon_r\varepsilon_0 = (\varepsilon'_r - j\varepsilon''_r)\varepsilon_0 = \varepsilon_0\varepsilon'_r(1 - j\tan\delta_\varepsilon)$ and magnetic constant (permeability) $\mu = \mu_r\mu_0 = (\mu'_r - j\mu''_r)\mu_0 = \mu_0\mu'_r(1 - j\tan\delta_\mu)$ of these materials (ε_0, μ_0 – parameters of the vacuum; $\tan\delta_\varepsilon$; $\tan\delta_\mu$ – dielectric and magnetic loss tangents; details in the next section). The real parts of the relative parameters (ε'_r; μ'_r) can have as positive, as well as negative values for different materials. Exactly this circumstance is the basis for the nowadays classification of modern materials [3, 4]. First of all, most of the standard dielectrics and some

magneto-dielectrics fall in the group of double-positive (DPS or right-hand) materials, for which $\varepsilon'_r > 0$; $\mu'_r > 0$. They still are the most occurring electro-dynamic media in modern electronics. The other two media are also well-known from nature: a group of the "epsilon"-negative (ENG) materials – $\varepsilon'_r < 0$; $\mu'_r > 0$ and group of the "mu"-negative (MNG) materials – $\varepsilon'_r > 0$; $\mu'_r < 0$. Many plasma media (ENG) and ferrites (MNG) at certain frequency intervals in external dc magnetic fields fall in the last two groups. The fourth group represents the double-negative (DNG or left-hand) materials – $\varepsilon'_r < 0$; $\mu'_r < 0$; this is the class of the most rapidly developing engineering artificial materials and negative reflective index meta-materials with very specific and extra-ordinary properties, not existing in nature, which gives us the right to call them 21st century electromagnetic and photonic materials, as it is pointed in [5].

2.2. DIELECTRIC AND MAGNETIC PROPERTIES OF MATERIALS

The complex permittivity ε_r of the materials in the microwave region varies between the static (dc) value ε_{dc} at very low frequencies up to the optical value ε_∞ at very high frequencies according to the empirical Cole-Cole model [6], often used to describe the dielectric relaxation in the water and polymers

$$\varepsilon_r \cong \varepsilon_\infty + \frac{\varepsilon_{dc} - \varepsilon_\infty}{1 + (j\omega\tau)^{1-\alpha}} . \qquad (1)$$

Exactly due to this reason the "microwave" complex permittivity $\varepsilon_{MW} = \varepsilon_r$ of the materials could be enough informative for the relaxation mechanism understanding, specific sample structure, used inclusions and other properties of the materials (ω is the angular frequency, τ – relaxation time; $\omega_r = 1/\tau$ – relaxation frequency; α is a parameter between 0 and 1; $\alpha = 0$ describes pure Debye relaxation model; $\alpha > 0$ – stretched relaxation model).

From a more common point of view, the "permittivity ε is a measure of how an electric field affects, and is affected by a dielectric medium, and is determined by the ability of a material to electrically polarize in response to the field, and thereby reduce the total electric field inside the material" [7]. It is directly related to electric susceptibility χ_e, which is a measure of how easily a dielectric polarizes in response to an electric field. They are related to each other through expression $\varepsilon_r = (1 + \chi_e)$, where ε_r is a scalar quantity in the very simple case of linear, homogeneous and isotropic materials, while when the medium is anisotropic, the permittivity is tensor $\tilde{\varepsilon}_r$.

By similar considerations, the permeability μ is the degree of magnetization that a material obtains in response to an applied magnetic field. The relative permeability $\mu_r = (1 + \chi_m)$ is related to the magnetic susceptibility χ_m, which is sometimes called volumetric or bulk susceptibility, to distinguish it from χ_p (magnetic mass or specific susceptibility) and χ_M (molar or molar mass

susceptibility). Again, μ_r is a scalar quantity for linear, homogeneous and isotropic magnetic materials, while when the medium is anisotropic (gyrotropic), the permeability is tensor $\tilde{\mu}_r$.

In general, as the permittivity $\varepsilon_r(\omega)$, as well as the permeability $\mu_r(\omega)$, are not constants; they both can vary with the local position in the medium, sample form (depolarization, demagnetization), the frequency of the fields applied (electric/magnetic), humidity, temperature, and other parameters. In the non-linear media, they may depend on the strength of the electric/magnetic field.

Most of the modern artificial materials could be considered as mixtures between two or more isotropic components. In this case, very important is the homogenization of the resultant material, which can be described by effective (we prefer to use the term "equivalent") dielectric or magnetic constant (ε_{eq}; μ_{eq}). The process of homogenization is possible to a certain extent degree [8] if the characteristic length of the non-resonant inclusions in the mixture is sufficiently smaller than the wavelength λ at the operating frequency (typically less than $\lambda/10$ to $\lambda/1000$). There exist many different technologies to mix two dielectrics: series, parallel, series-parallel; layered, dispersed (uniform or random), pillar, impregnated, foamed, woven, knitted, by additive or subtractive technology, etc. The question is how to calculate the resultant effective/equivalent parameters of the mixed material. There exist many different empirical formulas [9]; one of the earlier approximations is the well-known Maxwell-Garnett expression [7], when the mixture is got from small spherical dielectric inclusions of permittivity ε_2, embedded in a host environment medium of permittivity ε_1.

$$\varepsilon_{eq} = \varepsilon_1 + 3V_2\varepsilon_1 \frac{\varepsilon_2 - \varepsilon_1}{\varepsilon_2 + 2\varepsilon_1 - V_2(\varepsilon_2 - \varepsilon_1)}, \tag{2}$$

where V_2 is the normalized volume fractions of the inclusions; the total volume is $V_1 + V_2 = 1$. Close expression to the microwave substrates, textile fabrics, 3D printed and layered composites is the Wiener formula for laminar mixture [10]

$$\frac{1}{\varepsilon_{eq} + u} = \frac{V_2}{\varepsilon_2 + u} + \frac{V_1}{\varepsilon_1 + u}; \quad 0 \le u \le \infty, \tag{3}$$

where the parameter u depends of the orientation between the layers, namely:

$$\frac{1}{\varepsilon_{eq}} = \frac{V_2}{\varepsilon_2} + \frac{V_1}{\varepsilon_1};\ u = 0 \ (3.1); \quad \varepsilon_{eq} = \varepsilon_2 V_2 + \varepsilon_1 V_1;\ u = \infty \ (3.2); \quad u = \sqrt{\varepsilon_2 \varepsilon_1} \ (3.3)$$

for series layers (Reuss bound) (3.1); for parallel layers (Voigt bound) (3.2) and for isotropic mixtures with randomly arranged grains (Bruggman formula) (3.3) – see the illustration curves in Fig. 2.1*a*,*b* [A52].

The effective (equivalent) media models are very important for the characterization of the different mixed dielectrics. They present the difference between

the pure parallel and pure perpendicular to the E-field direction dielectric inclusions. There exist two main ways to realize multi-component isotropic (homogenized) dielectrics with well-designed dielectric constant: 1) by random mixing (as for the foams) or 2) by constituents with similar dielectric parameters (as for the microwave substrates and woven/knitted textile fabrics). However, in the case of 3D printing, these methods are not fully applicable; here we should use symmetrical unit cells for the infilling medium (see [2]).

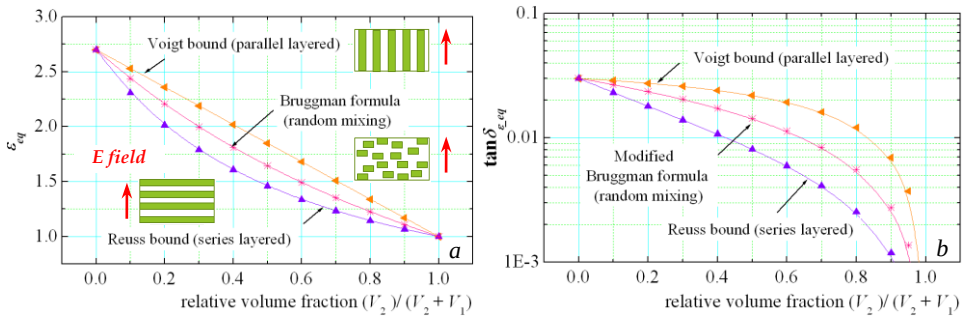

Fig. 2.1. Minimal and maximal bounds for the resultant equivalent dielectric constant (*a*) and dielectric loss tangent (*b*) of two mixed dielectrics [A54]

The next step for generalization of the concept for the electromagnetic material constants is the introducing of resonance effects in the permittivity and permeability behaviour. In the dielectric materials, the charges are displaced by an incident electric field. The amplitude is given by the restoring forces on the electrons and depends strongly on the time-variation of the field and this dipole (formed by the displaced electrons and the remaining ion) will oscillate. For frequencies around a certain frequency ω_0 the induced dipole moment might be very large and strongly depend on the frequency. This increasing interaction (called "resonance") of the incident electromagnetic field with the structure will lead to strong scattering and absorption. The behaviour of the oscillating dipole can be described on the base of a simple driven harmonic oscillator and the solution gives the known relation between the polarization P and electric field E expressed by the electric susceptibility χ_e, namely $P = \varepsilon_0 \chi_e E$. The solution to the differential equation describing forced resonance is governed by a complex Lorentzian function. Taking in mind that the electric displacement D is related to the polarization density P by $D = \varepsilon_0 E + P = \varepsilon_0 (1+\chi_e) E = \varepsilon_r \varepsilon_0 E$, the effective/ equivalent resonance dielectric constant by the Lorentz model is [7, 8]:

$$\varepsilon_{eq}(\omega) = 1 + \frac{\omega_p^2}{\omega_0^2 - \omega^2 - j\omega\gamma_e}; \quad \omega_p^2 = \frac{Nq^2}{\varepsilon_0 m_e}, \tag{4}$$

in which ω_0 is the natural resonance frequency, ω is the operating frequency, ω_p is the so-called plasma frequency and γ_e is the damping factor in [loss/s] (here

also N is the number of atoms per unit volume, q is the unit charge, m_e is the effective electron mass). This model can be generalized for multiple resonances.

By a similar way, a Lorentz model can be introduced for permeability [11]:

$$\mu_{eq}(\omega) = 1 + \frac{F\omega^2}{\omega_{m0}^2 - \omega^2 - j\omega\gamma_m}, \tag{5}$$

where now ω_{m0} is the magnetic resonance frequency (when the magnetic element is the widely used for metamaterials' construction split-ring resonator SRR [12]), γ_m is the magnetic damping factor, and F is a parameter that depends on the loop gap in the SRR.

Both expressions (4, 5) show that the materials can have at some frequency intervals either positive or negative values for the effective/equivalent dielectric and magnetic constants, or even double negative values (DNG) – see examples on Fig. 2.2*a*,*b*. This approach is widely used in modern metamaterial design [13]. Due to these reasons, some other parameters, which describe the metamaterials, can have anomalous behaviour. For example, the refractive index n may obtain negative signs for some metal-content metamaterials [8] (for isotropic and linear media the simple expression is $n = \sqrt{\varepsilon_r \mu_r}$).

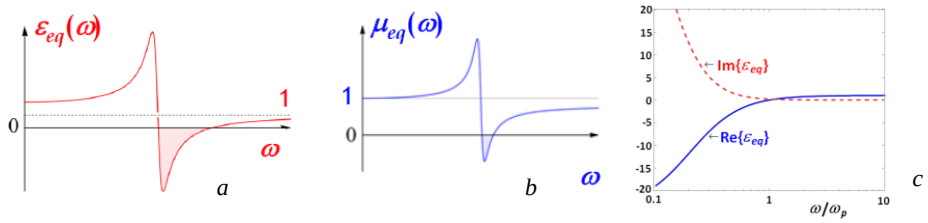

Fig. 2.2. Illustration of possible frequency behaviour of the real effective (equivalent) dielectric ε_{eq} or magnetic μ_{eq} constants for (*a*) artificial dielectrics and (*b*) artificial magnetics with resonance behaviour; (*c*) the real (solid blue) and imaginary (dashed red) parts of the relative permittivity as functions of frequency for an example material following the Drude model [6]

For the special case of metals, the Lorentz model transforms into the Drude model. In metals, most electrons are free because they are not bound to nuclei (the restoring force is negligible and the natural frequency $\omega_0 = 0$ in (4)); therefore they will oscillate harmonically under the influence of an incident electromagnetic wave and this can be described by an oscillating current density $J = \sigma E$ (for linear media), where σ is the conductivity. Taking in mind the relations between the polarization P, current J and electric field E [7], we can introduce a more common definition for the relative equivalent permittivity (so-called relative generalized permittivity $\hat{\varepsilon}_{eq}(\omega)$):

$$\hat{\varepsilon}_{eq}(\omega) = \varepsilon_{eq}(\omega) - j\sigma_{eq}(\omega)/\omega, \tag{6}$$

where the equivalent complex quantity $\varepsilon_{eq}(\omega)$ measures the polarization response due to bound charges, and $\sigma_{eq}(\omega)$ is the equivalent conductivity, taking in mind the response of the free charges. Thus, the generalized permittivity in conductors has a large imaginary part (the second term in (6)) and this means that the losses are large. But this also means that the penetration depth δ of the electromagnetic waves into the sample surface is small. The fields attenuate rapidly within the conductor and the fields are confined to a thin surface layer; this allows the definition of surface current and surface impedance, often used by the electronics and electrical engineers. Fig. 2.2*c* displays the frequency behaviour of the permittivity in the Drude model. As can be seen, at low frequencies the imaginary part dominates the response. Indeed, the typical conductivity behaviour for metals at low frequencies $\hat{\varepsilon}_{dc}(\omega) \to -j\sigma_{dc}(\omega)/\omega$ is included in the Drude model in the limit $\omega \to 0$, and the limit for the dc conductivity is $\sigma_{dc} = \omega_p^2 \varepsilon_0 / \gamma_e$. The Drude model is often used to describe the optical properties of noble metals, from which most optical metamaterials are made.

All the considered approximations, models and expressions above clearly show that the material constants are well determined by the overall structure of the samples and their interaction with the EM waves, by the type of components in the resultant complex mixtures, by orientation and position of the building blocks and applied technology. The specific integral character of the equivalent material constants (ε_{eq}, μ_{eq}) gives a potential to ensure additional information for the material properties to the results, already obtained by different local methods (e.g. spectroscopy) that are widely used for their characterization. In this paper, we concentrate our efforts exactly over the reliable characterization of the material constants (mainly permittivity) in the microwave range as an electromagnetic representative of the materials in different electrodynamic projects. Moreover, the electromagnetic response depends also on the material anisotropy.

2.3. ANISOTROPY AND ORIGINS OF THE ANISOTROPY IN MODERN ARTIFICIAL MATERIALS.

The electromagnetic anisotropy of materials can be expressed as the existence of different dielectric/magnetic constants in different directions. The reasons could be quite different. The microwave and optical engineers usually connect the anisotropic behaviour with the microwave ceramics and optical lenses; this is one of the oldest known types of material anisotropy, named crystalline anisotropy for single- or poly-crystalline materials (optical glasses, ceramics, artificial soft and low-temperature co-fired ceramics LTCC, liquid crystals, etc.). In principle, these materials are homogeneous, but the anisotropy appears due to the existence of different crystallographic axes in the lattices and the fact that charges oscillate differently along these directions. This anisotropy is usually relatively strong. Our early investigations were connected exactly with this type of anisotropy of ceramic disks, cylinders, rings and rods by different microwave

methods [A1, A2, A4, A7]. Then the characterization of crystalline and crystalline-like materials continued by the two-resonator method [A35, A55, A58].

Another specific group of plasma/ferrite researchers identify the original concept for the material anisotropy with the electric or magnetic gyrotropy of gaseous or solid-state plasmas (gyro-electric) and ferrites (gyro-magnetic), all in external dc magnetic biasing fields. These phenomena belong to the so-called induced anisotropy; the dielectric and magnetic properties of such natural metamaterials have been described with a non-symmetric tensor form of the permittivity and permeability (including non-diagonal components, controllable by external dc biasing magnetic field). The ferroelectric materials and films can also be associated with this group of electrically gyrotropic materials but in the external dc electric biasing field. In our early investigations, we performed a lot of attempts for difficult characterization of the microwave ferrites with different forms: disk, rod, cylinder, prism [A3,A4,A7];we applied successfully these results in our models and methods of design of different gyrotropic devices – circulators and isolators (see the review papers [A5,A6]). Special types of investigations were devoted to ferrite and magneto-dielectric thin films [A16,A17,A24] and microwave absorbers [A11,A29,A52]. Our contribution to the characterization of gaseous plasma media was connected with the development of classical and new types of hairpin resonance probes for the determination of plasma density[A28,A36,A38]

Nowadays, a new class of artificial materials appeared, for which the measured anisotropy could be considered more as an undesired property. First of all, in this group, we can add the commercial engineered reinforced substrates with many applications in the modern RF and microwave electronics. Characterization of the dielectric anisotropy of such popular materials is very important for the reliability of the modern design of different planar structures on high-frequency substrates, especially in the millimetre-wave range. Our research is connected mainly with the characterization of these commercial materials ([A9-A14, A18, A19, A21-A23, A25, A27, A31-A33, A35, A37, A41, A43, A45, A46], see also [2]). In our practice we measure reinforced substrates from different manufacturers, which anisotropy varies in a wide range: from ~1-2 % up to 25 % (see below for this parameter) [A32]. The anisotropy of similar structures has been caused by the spatial inhomogeneity in different directions between the mixed reinforcing fibres net and the applied filling. To this group of anisotropic materials we can add the textile fabrics [A50] used for wearable antennas, multilayer antenna radomes [A15,A20,A26], some 3D printed dielectrics [A48,A54,A55].

The controllable anisotropy of the engineered metamaterials and “bandgap” materials (i.e. controllable dielectric constants in different directions) is another new type of artificial anisotropy [8, 14], caused by the chosen shape, geometry, size, orientation and arrangement of the unit cells, which form the “lattice” of the artificial materials. Extremely big could be the anisotropy of metamaterials with metal inclusions. Therefore, it is very similar by origin with the anisotropy, caused from the inhomogeneity of the reinforced and composite samples, but

now this property is well-designed and fully desired, because it ensures unusual characteristics of some anisotropic metamaterial devices [16]: invisible cloaks, wave concentrators and converters, superlenses, special sensors, etc. We already started characterization of such metamaterials with big anisotropy [A49, A53].

Let's consider the terminology, connected with the anisotropy. In the common case, the anisotropic/gyrotropic materials are describing by full tensors; the material tensors are non-symmetrical for ferrites and plasma [8]; but they will not be considered in the paper. There exist three cases of so-called dielectric anisotropy of the artificial materials, which dielectric constants can be described by diagonal tensors, namely: bi-axial (6.1) and uni-axial anisotropy (6.2) or pure isotropy (6.3) (similar expression could be written for the magnetic constants):

$$\left(\hat{\varepsilon}_r\right)=\begin{pmatrix}\varepsilon_{xx} & 0 & 0\\ 0 & \varepsilon_{yy} & 0\\ 0 & 0 & \varepsilon_{zz}\end{pmatrix}\ (6.1);\quad \left(\hat{\varepsilon}_r\right)=\begin{pmatrix}\varepsilon_{par} & 0 & 0\\ 0 & \varepsilon_{par} & 0\\ 0 & 0 & \varepsilon_{perp}\end{pmatrix}\ (6.2);\quad \left(\hat{\varepsilon}_r\right)=\begin{pmatrix}\varepsilon & 0 & 0\\ 0 & \varepsilon & 0\\ 0 & 0 & \varepsilon\end{pmatrix}\ (6.3)$$

$$\varepsilon_{xx}\neq\varepsilon_{yy}\neq\varepsilon_{zz};\qquad \varepsilon_{par}=\varepsilon_{xx}\approx\varepsilon_{yy};\quad \varepsilon_{perp}=\varepsilon_{zz};\qquad \varepsilon_r\approx\varepsilon_{xx}\approx\varepsilon_{yy}\approx\varepsilon_{zz}$$

Typical bi-axial anisotropic materials are the crystals, optical glasses, liquid crystals, thin films and nanostructures, many metamaterials with non-symmetrical unit cells, 3D printed dielectrics, textile fabrics, plant and other bio-tissues, which can be described with three different scalar dielectric constants along the axes 0*x*, 0*y* and 0z. The uni-axial anisotropy has been expressed in relatively thin structures with plane symmetry, e.g. materials like the reinforced substrates,hard or soft artificial ceramics, LTCC's, single or multilayer antenna radomes, some gradient dielectrics and absorbers. The near-to-isotropic behaviour is a property of the homogenized and foam-like materials and metamaterials: foams, bulk plastics, injection-moulded dielectrics, non-woven substrates, foamed absorbers,etc. In the second part of this paper [2], we will consider many concrete examples.

Finally, the so-called magneto-electric materials appear among modern artificial materials [7, 16]. The common issue for these materials is the magneto-electric coupling; now, the complex electric and magnetic flux densities $\vec{D}$ and $\vec{B}$ in the so-called bi-anisotropic magneto-electric materials can be expressed as

$$\vec{D}=\left(\hat{\varepsilon}\right)\vec{E}+\left(\hat{\xi}\right)\vec{B}\qquad (7.1)\quad \text{and}\quad \vec{B}=\left(\hat{\mu}\right)\vec{H}+\left(\hat{\zeta}\right)\vec{E}\qquad (7.2)$$

where $\left(\hat{\varepsilon}\right)$, $\left(\hat{\mu}\right)$ are the permittivity and permeability tensors, while $\left(\hat{\xi}\right)$, $\left(\hat{\zeta}\right)$ are tensors of the corresponding magneto-electric coupling coefficients. When the parameters ε, μ, ξ, ζ are scalars, the materials become bi-isotropic. The above relations show that the equivalent permittivity in such materials can depend not only on the response to the E field but also on the response to the H field in the considered media (v.v. for permeability). We already managed to measure in our practice such samples [A53, A60-A63], but this research is in the beginning.

2.4. NUMERICAL METHOD FOR ANALYSIS OF DIELECTRIC ANISOTROPY IN ARTIFICIAL MATERIALS

The discussions in the previous section express the importance of anisotropy for any artificial material, not only for metamaterials. Therefore, it is important to may predict the degree of anisotropy in different materials, but this is not possible in all cases. The full-wave analysis of anisotropic structures is possible in a few simple cases. The anisotropy type of materials with crystalline structure can be bound to the lattice symmetry – isotropy for crystals with cubic symmetry; uni-axial anisotropy – with hexagonal, tetragonal symmetry; bi-axial anisotropy – with monoclinic, triclinic, orthorhombic symmetry [8]. Another very popular model for crystalline anisotropy in high-ε ceramics is based on the lumped-element approach: the building blocks as electric dipoles can be considered at the macroscopic level as a set of parallel or series capacitors (for example see the expressions 3.1-2), but the calculated anisotropy is usually bigger than the measured one. Unfortunately, the other effective-media expressions for the resultant permittivity in different mixtures cannot give the actual anisotropy [9, 10]. There exist also attempts to bind the degree of symmetry of the unit cells for evaluation of the all-dielectric 3D printed metamaterials [8, 14]. Of course, the numerical simulations by the nowadays 3D EM simulators are also widespread; many microwave and optical engineers successfully apply this approach, and therefore, the big software developers pay serious attention the new versions of the commercial 3D simulators to may cope fluently with the metamaterials.

In [A48, A50, A54] we proposed a numerical method for reliable prediction of the dielectric constants of artificially-constructed materials (incl. all-dielectric metamaterials or even samples with metal inclusions) along to all three axes in the Cartesian system by resonance method in desired frequency intervals. The idea of this method is to build a well-designed unit cell, to reproduce it in a hosting isotropic substrate and to put the whole sample in a rectangular resonator (Fig. 2.3), which supports TE and TM modes with three mutually perpendicular directions of the E fields – see illustrations in Fig. 2.4.Independent extraction of the resultant dielectric constant along all three axes is possible after replacing of the bi- or uni-anisotropic sample under interest with an equivalent isotropic sample. We successfully applied the described method for many artificial samples: textile fabrics [A49], 3D printed dielectrics [A54, A56], metamaterials with surface metal inclusions [A48, A53]. Different unit cells could be used for these numerical investigations: spheres, cubes, cylinders, prisms, disks and some combinations between them, made by isotropic dielectrics or by metals. We use for a quantitative measure of the resulting dielectric constant/loss tangent anisotropy (parameters ΔA_{ε}, $\Delta A_{\tan\delta\varepsilon}$) for bi-/uni-axial anisotropy the following expressions

$$\Delta A_{\varepsilon,0x/y} = 2(\varepsilon'_{0x/y} - \varepsilon'_{0z}) / (\varepsilon'_{0x/y} + \varepsilon'_{0z}), \tag{8.1}$$

$$\Delta A_{\tan\delta\varepsilon,0x/y} = 2(\tan\delta_{\varepsilon,0x/y} - \tan\delta_{\varepsilon,0z}) / (\tan\delta_{\varepsilon,0x/y} + \tan\delta_{\varepsilon,0z}), \tag{8.2}$$

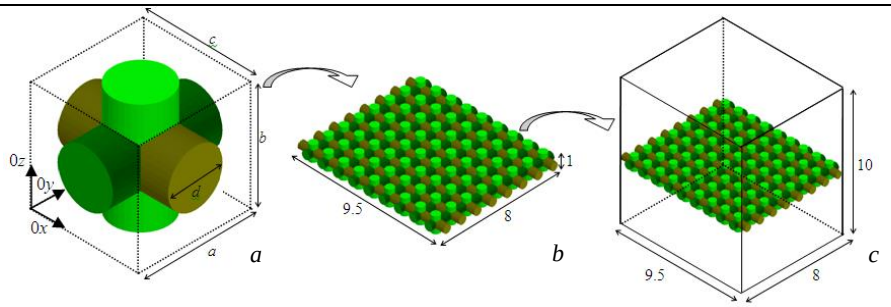

Fig. 2.3. (*a*) Universal unit cell; (*b*) constructed artificial sample with repeated unit cells (inclusions) in a hosting isotropic substrate; (c) artificial sample in a rectangular resonator

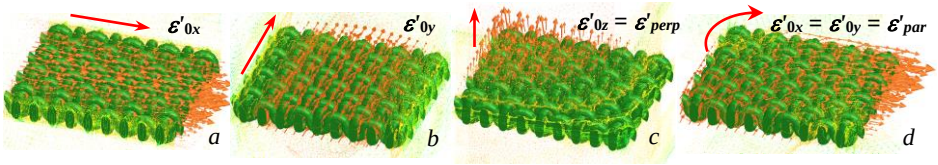

Fig. 2.4. Rectangular resonator with an artificial sample, which supports different modes with mutually perpendicular E fields along the axes: (*a*) 0*x*; (*b*) 0*y*; (*c*) 0*z* and (*d*) 0*xy*

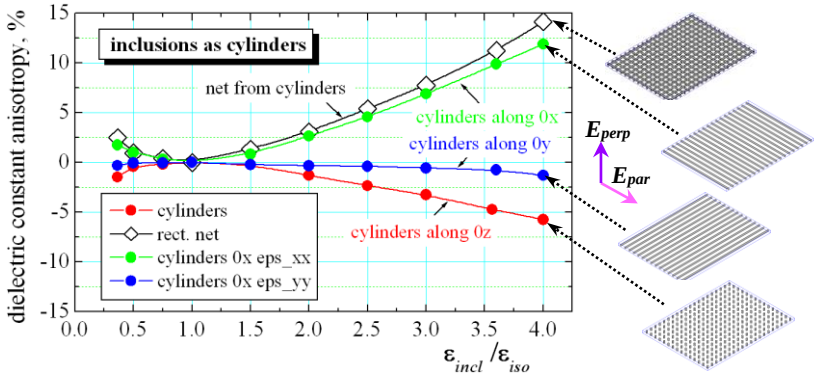

Fig. 2.5. Dielectric constant anisotropy of net from simple inclusions as cylinders, orientated along to 0*x*, 0*y*, 0*z* and 0*xy*; the E-fields orientation is fixed either along to 0*x* (E_{par}) or along to 0*z* (E_{perp})

The dependencies for A_ε, % versus the ratio $\varepsilon_{incl}/\varepsilon_{iso}$ in Fig. 2.5 well illustrate a simple but informative case for anisotropy prediction: inclusions as dielectric cylinders with permittivity ε_{incl} orientated along the axes 0*x*, 0*y* and 0*z*, keeping the E fields parallel or perpendicular to the sample surface by exiting fixed mode in the rectangular resonator (ε_{iso} is the permittivity of the hosting medium). The simulations show that the resultant permittivity $\varepsilon_{par,0x}$ of the artificial mixture increases along to the cylinders when the E field is orientated along to the same axis, in comparison to the dielectric constant $\varepsilon_{par,0y}$, perpendicularly to the cylinder axis. This effect increases the anisotropy $A_{\varepsilon,\ 0x}$ of the whole artificial substrate along to the cylinder axis with the rise of ratio $\varepsilon_{incl}/\varepsilon_{iso}$, while the anisotropy $A_{\varepsilon,\ 0y}$ is close to zero. The effect of anisotropy for $\varepsilon_{incl} \rangle\rangle\ \varepsilon_{iso}$ increases for net of cylinders. The positive ΔA_ε sign means that $\varepsilon_{par} > \varepsilon_{perp}$, while the

negative sign – that $\varepsilon_{par} < \varepsilon_{perp}$. The last effect happens, when the cylinders are orientated perpendicularly to the sample. The presented above investigations have been not published jet, however, we confirmed numerically and experimentally the described rules for anisotropy of textile fabrics [A50], reinforced substrates [A32], multilayer antenna radomes [A15,A26], 3D printed dielectrics [A56], metamaterials [A48]. Similar investigations are helpful for the design of homogenized and near-to-isotropic 3D printed dielectrics for antenna applications [A54] (see also [2] for more details)

3. METHODS FOR CHARACTERIZATION OF DIELECTRIC PROPERTIES OF DIFFERENT MATERIALS IN THE MICROWAVE RANGE.

Nowadays a lot of measurement methods exists for characterization of artificial materials, some of them reference (approved from the leading world standardization organizations as IPC, NIST, NPL [17-19]), or developed by different Universities and science organizations. This is a world wealth, nevertheless that some methods can give different results for the same materials. Three types of methods can be classified in the microwave range: free-space, waveguide (transmission-line) and resonance methods – Fig. 3.1*a*-*d*. The first two are considered as broadband, but less accurate methods, while the resonance methods are specified as more accurate, but narrowband ones. A good survey of the microwave methods for material characterization has been done in [20]. We consider selectively in this paper the promising methods with an accent to these, which can measure anisotropy and have been already realized in the Microwave Lab in the Faculty of Physics of Sofia University "St. Kliment Ohridski" [1].

3.1. RESONANCE METHODS.

Definitely, the resonance methods are considered more accurate than the transmission-line methods [21].The main reason is the fact that the sample under interest is a part of bigger resonance area (Fig. 3.1*d*) and its dielectric and/or magnetic constants influence relatively strongly the resonance parameters of the excited modes – resonance frequency f_0 and unloaded quality factor Q_0 of the empty resonator, shifting them to f_ε and Q_ε, when the sample is placed inside (in the case of volume resonators; in other cases the sample itself could be a high-Q resonator). The big accuracy is achieved since the frequency or frequency

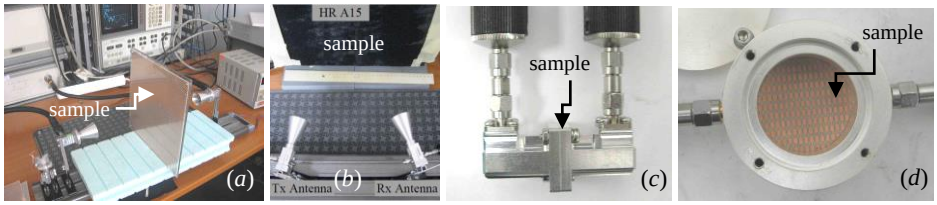

Fig. 3.1. Three popular methods used for characterization of flat samples: (*a*) free-space method in transmission regime; (*b*) in reflection regime; (*c*) waveguide method; (*d*) resonance method

differences can be measured with small errors in the microwave range, typically less than 0.01% in the X band. However, other factors can decrease the measurement accuracy: actual sample shape and sizes, sample positioning in the resonator, environmental factors, etc. Our short survey of the resonance methods will be concentrated over their ability to measure the sample anisotropy (8.1-2).

A measurement resonator can detect and extract the sample anisotropy if it supports at least three modes with mutually perpendicular E (or H) fields along the Cartesian axes in a given frequency interval. A good illustration is the resonance perturbation method [22], suitable for characterization of the biaxial anisotropy of liquid crystal polymers (LCP), which have serious potential for application in the modern microwave electronics. The method uses three modes TE_{011}, TM_{120} and TE_{101} with mutually perpendicular E-field orientations in a non-standard rectangular cavity (Fig. 3.2*a*) to extract the permittivity values ε_{xx}, ε_{yy} and ε_{zz}. We apply rectangular resonators made by standard waveguides that support dominant modes TE_{10p} (p = 1-6), to extract either dielectric or magnetic parameters of microwave absorbers (Fig. 3.2*b*). Due to the coarse character of the known perturbation expressions [20],we apply more accurate 3D simulations.

The volume resonators also have good potential to determine the sample anisotropy, but here is no universal solution. The parallel dielectric parameters $\varepsilon_{par}/\tan\delta_{\varepsilon,par}$ can be measured by TE-mode resonators (as R1 in Fig. 3.3*a*) (classical Courtney's method [23], Kent's evanescent-mode tester [24], split-cylinder resonator SCR [25], split-post dielectric resonator [26], etc.). The perpendicular parameters $\varepsilon_{perp}/\tan\delta_{\varepsilon,perp}$ can be estimated by TM-mode resonators (as R2) (e.g. as in [A21, 27], reentrant cavities [28]). In fact, only a few publications have been directly dedicated to anisotropy measurements. Whispering-gallery modes with high-azimuthal index in a single dielectric resonator with fields far from the screens could be used for anisotropy measurement of ultra and extremely low-loss materials [29].The method presented in [30] is based on resonance measurements of one prism sample in three mutually perpendicular orientations in a rectangular resonator (as in [A55, A58] for cylindrical resonators). Very important is the problem for reference determination of the proven dielectric anisotropy of the commercial microwave substrates, because the reference IPC TM-650 2.5.5.5 [17] (clamped stripline resonator test method) cannot give this parameter. The modified IPC TM-650 Bereskin's method [31] is difficult for realization (many substrates have to be stacked horizontally and then a single sa-

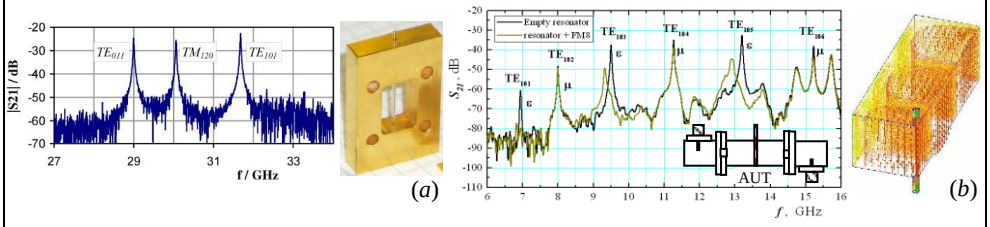

Fig. 3.2. Perturbation resonance method: (*a*) for determination of biaxial anisotropy of LCP [22]; (*b*) for separate determination of dielectric and magnetic parameters of microwave absorber [A29]

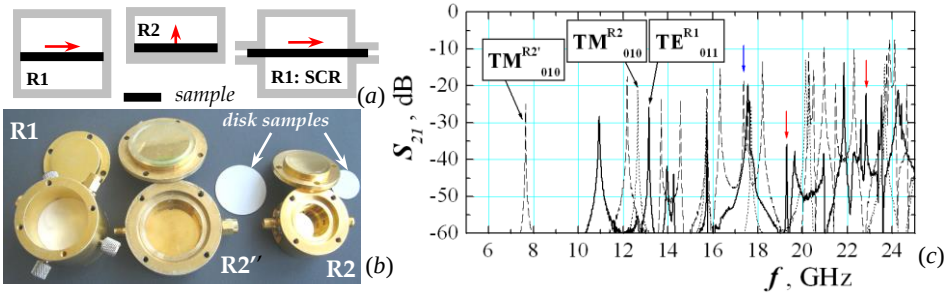

Fig. 3.3. (*a*) TE- (R1; SCR) and TM-mode (R2) cylindrical resonators; (*b*) pairs with equal diameters (R1&R2') or with equal resonance frequencies (R1&R2); (*c*) mode spectrum (0-25 GHz)

mple has to be produced by a vertical cut); only a few substrate producers apply this method. Nowadays, a broadband method is proposed [32],based on numerical extraction of the parallel and perpendicular dielectric constants from data for the even and odd modes in coupled microstrip resonators printed on the substrate under test. However, the authors make a wrong conclusion about the ability to determine the parallel permittivity of a substrate (in fact, they determine the so-called design or microstrip-like value and this is proven by our measurements). Similar to the Bereskin's method (in stripline geometry) is the method, proposed in [33] and implemented by substrate-integrated waveguide (SIW) resonators. The novelty here is the possibility to increase the working frequency up to mm-wavelength range. A common disadvantage of the methods, based on the printing of measurement resonators on the substrate under test, is the difficult extraction of the dielectric loss tangent of raw substrates by taking into account the influence of the quality of metallization (the problem is discussed in §3.3). Recently, a new TM-mode method (balanced-type circular disk resonator [34, 35]) shows potential for characterization of perpendicular dielectric parameters of flat samples up to 110 GHz (now reliable results have been obtained in the interval 20-70 GHz). We just started to develop this method to help substrate anisotropy determination in the frequency bands for 5G standard. Combined with the free-space or open-resonator method for determination of the parallel dielectric parameters (considered in §3.3), they both can be a good base for characterization of material anisotropy up to the mm- and sub-mm wavelength range.

3.2. CHARACTERIZATION OF THE DIELECTRIC ANISOTROPY OF MATERIALS BY THE AUTHORSHIP TWO-RESONATOR METHOD AND ITS MODIFICATIONS

In 2000-2002 we first detected the dielectric anisotropy of commercial microwave substrates and developed an authorship method for its determination – the two-resonator method [A22]. The first publications [A8, A12] have been based on a perturbation approach, but then we developed more accurate full-wave analytical models of the measurement resonators and for the extraction procedure of the complex dielectric constants of uni-axial anisotropic single and multilayer samples [A18, A22, A27]. Applying this method we managed to

accumulate in a short period (2004-2008) a tremendous amount of data for the real anisotropy on many commercial substrates from different producers (used in our antenna projects [A30, A34, A39-A41, A45, A59, A63]. However, we have encountered many difficulties for a long time in trying to impose the idea of having such a feature (anisotropy) of these most spread electronic components (micro-wave substrates) as among the big substrate producers, as well as among the most of the users (we discuss this "story" for the substrate anisotropy in [2]).

The two-resonator method [A22, A32] is based on two consecutive measurements with/without samples of the resonance characteristics of two symmetrical modes: TE_{011} in R1 resonator (with E fields parallel to the substrate) and TM_{010} in R2resonator (E fields perpendicular to the substrate) – Fig. 3.3*a* and Fig. 3.4*a*. To achieve the best sensitivity of this method the sample is placed in the middle of R1, while it lies on the resonator bottom in R2; the chosen lower height H_2 of R2 well separates the TM_{010} and TE_{011} resonances. The method can be realized in two options: 1) for samples with equal diameters $D_1 = D_2$ (e.g. 30 mm), but the TM_{010} mode has lower resonance frequency (7.65 GHz) than for TE_{011} mode (13.15 GHz); or 2) for achieving of close resonance frequencies (e.g. in the interval 12.6-13.15 GHz), but applying resonators with different diameters (D_1 = 30 mm; D_2 = 18.1 mm) – see the examples in Fig. 3.3*b*,*c*. The considered here frequency band of the described method can be expanded to higher frequencies by using several selected high-order modes: e.g. TE_{013}, TE_{021}, TE_{031} in R1 and TM_{020}, TE_{030} in R2; however, they should be well-identified in the mode spectrum (see the modes marked with arrows in Fig. 3.3*c*). The other way for frequency range widening is to increase or decrease the resonator (and sample) diameter. The diameter decreasing can increase the operating frequencies (e.g. for TE_{011} in R1: f_1 ~ 21.8 GHz at D_1 = 18.1 mm; f_1 ~ 28.7 GHz at D_1 = 15.0 mm; f_1 ~ 39.3 GHz at D_1 = 10.0 mm; for TM_{010} in R2: f_2 ~ 22.8 GHz at D_2 = 10.0 mm; f_2 ~ 28.5 GHz at D_2 = 8.0 mm; by higher-order modes in R1: up to 70-80 GHz; in R2: up to 65-70 GHz). However, the decreasing of resonator diameter leads to a decreasing of measurement accuracy, especially for the dielectric loss tangent, due to the smaller volume and lower Q factors in both resonators.Conversely,the diameter increasing leads to resonance frequency decrease and we managed to determine the substrate anisotropy by measurements even at 1.4-2.5GHz [A50], but the sample sizes become too big and the accuracy again decreases. There is another way to decrease the frequency interval for anisotropy determination by

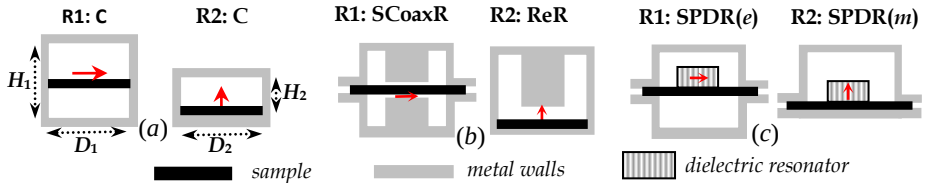

Fig. 3.4. Two-resonator method, realized by three different pairs of TE/TM resonators: (*a*) cylinder resonators (R1:C or R1:SCR and R2:C); (*b*) split coaxial resonator (R1:SCoaxR) and re-entrant resonator (R2:ReR); (*c*) split post dielectric resonators (R1:SPDR(*e*) and R2:SPDR(*m*))

by small samples – to use another pair of R1/R2 resonators with naturally lower resonance frequencies based on split-coaxial resonator as R1 [A25] and reentrant resonator as R2 [A23] – see Fig. 3.4*b*. With this new pair of resonators, we again decreased the frequencies for determination of substrate anisotropy to 1.7 GHz. In general, we successfully widened the applicability of two-resonator method by introducing in [A31, A32] the approach to use different pairs of measurement resonators from type R1/R2 and to obtain unique results for many commercial substrates, which was notified in [37, 38]. The third pair with split-dielectric post resonators SPDR(*e/m*) with TE/TM modes with added substrate sample allows us preliminary to choose a frequency for measurements by the used high-Q dielectric resonators (Fig. 3.4*c*). We successfully applied the authorship two-resonator method for many different materials excepting the microwave substrates, like multilayer composites, thin films, 3D printed dielectrics, textile fabrics, and even metamaterials (with less success) – details are discussed in [2].

The measurement errors of the two-resonator method have been estimated in [A22] as ~2.5-3% for ΔA_{ε} and ~10-12% for $\Delta A_{\tan\delta\varepsilon}$ in the case of multilayer materials in the Ku band (or 1.5% and 8-9% for single-layer substrates). These values fix the margins for determination of the practical isotropy of materials by the two-resonator method. A big contribution to the improvement of measurement accuracy is the concept for the equivalent parameters of measurement resonators [A31, A32]. Usually, the calculated and measured resonance parameters of the empty resonator do not fully coincide, $f_{0calc} \neq f_{0meas}$, $Q_{0calc} \neq Q_{0meas}$; the reasons are different: size uncertainty, the influence of the coupling loops, tuning screws, eccentricity, surface cleanness and roughness, daily temperature variations, etc. The problem can be overcome namely by the introduction of equivalent resonator dimensions and wall conductivity. The equivalent geometrical parameters (*D* or *H*) could be chosen on the base of a simple rule: the variation of which parameter influences more the resonant frequency of the empty cavity without any details? In the case of circular resonators the diameter changes "produce" bigger variation for the resonance frequency and Q factor (see dependencies in Fig. 3.5). If we tune the selected equivalent parameters in the constructed stylized 3D models of empty resonators, we can achieve practical coincidence between the calculated and the measured resonance parameters: $f_{0calc} \sim f_{0meas}$,

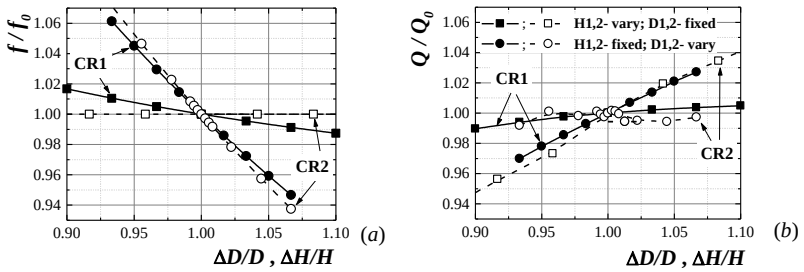

Fig. 3.5. Dependencies of the normalized resonance frequency (*a*) and normalized Q-factor (*b*) of the dominant mode in the cylinder measurement resonators CR1 and CR2

$Q_{0calc} \sim Q_{0meas}$. Thus, in the case of pair of cylinder resonators R1/R2 their 3D models include equivalent diameter $D_{eq1,2}$ (instead $D_{1,2}$), actual height $H_{1,2}$ and equivalent wall conductivity $\sigma_{eq1,2}$. Additional equivalent parameters could be introduced for the other two pairs of used resonators [A32].

3.3. FREE-SPACE AND WAVEGUIDE (TRANSMISSION-LINE) METHODS

The measurement setup of the free-space method (in transmission or in reflection regimes), consists of two or one horn antennas and the flat sample is between them or between the antenna and a reflecting screen – see Fig. 3.1*a,b*. The measurements of the phase delay and the losses with and without sample allow extracting the dielectric constant and dielectric loss tangent. This method is very useful for measurements in the mm- and sub-mm-wave ranges but needs relatively big samples to avoid the diffraction effects near to the sample edge. The main problems are the reducing of the measurement errors due to multiple reflections and sample misalignment. By suitable extraction procedure, these errors could be reduced or measurements in a TDR gate could be used. Due to the TEM mode propagating in the structure, it can be used for extraction only of the parallel dielectric parameters of the sample in a transmission regime.The method is not well applicable for low-loss materials, but it is very popular for characterization of new unknown materials, including metamaterials [A53, A60-61], composite materials as antenna radomes [A20, A26, A33] and absorbers [A29, A52, A63], all realized in our laboratory from X to Ka bands. An alternative of the free-space method is the resonance quasi-optical (Fabry-Perot) interferometer, realized in our laboratory in Ka-band; it can measure the parallel dielectric parameters in mm- and sub-mm wavelength ranges even for low-loss materials.

The waveguide methods are also very popular in the dm-, cm-, mm-wavelength ranges and beyond applying rectangular, circular or coaxial waveguides in transmission or reflection regimes. For rectangular waveguide in transmission regime, the thin sample can be placed between two waveguide flanges (as in Fig. 3.1*c*) or into the waveguide fitting its cross-section; the measurement of phase delay and insertion losses allows extraction of the sample dielectric parameters. Inserted in the waveguide aperture bulk samples can act as resonators in the corresponding frequency range; the extraction of the dielectric parameters is possible by measurement of the resonance frequency and Q factor. For thin samples in reflection regime, both dielectric and magnetic parameters can be extracted if the sample is placed in two fixed positions at a quarter-wavelength distance. When the sample is placed in the natural vertical position according to the wider wall of the waveguide, the method gives the parallel dielectric parameters; if the sample lies horizontally on this wall, the method extracts the perpendicular parameter. Thus, the waveguide method is one of the few relatively broadband methods, which can determine the anisotropy of the sample. Due to this reason, it is very popular for characterization of 3D printed metamaterials (e.g. see [14]), including in our laboratory [A29, A53].

The waveguide method can be also realized by planar transmission lines, printed on the substrate under interest. In this variant, it is known as differential phase length (DPL) method and it is one of the most spread methods for microwave substrate characterization on the base of microstrip lines (MSL). The realization is simple: S_{21} parameters of two or more 50-Ohms MSL (or other planar lines) with different lengths have been measured and phase difference $\Delta angS_{21}$, deg and difference between the insertion losses ΔS_{21}, dB have been determined for each pair of lines with length difference ΔL (Fig. 3.6*a*). Then the important parameters, effective dielectric constant ε_{eff} and attenuation α, can be calculated:

$$\varepsilon_{eff} = \left(\frac{\Delta \text{ang} S_{21}.c}{360\, f \Delta L} \right)^2, \qquad (8.1) \qquad \alpha, \text{dB/cm} = \Delta S_{21}, \text{dB} / \Delta L, \text{cm}. \qquad (8.2)$$

Fig. 3.6*b*,*c* presents an example for measured amplitude and phase S_{21} dependencies for a selected real commercial substrate (conditionally marked as "Substrate 3.0") of thickness 20 mils with catalogue dielectric constant 3.0. Using the corresponding measured differences in (8.1-8.2) for MSL on this substrate with different thicknesses (5, 10, 20 and 30 mils) new dependencies for the effective dielectric constant and attenuation for this substrate can be obtained – shown in Fig. 3.7. In addition to the DPL method, other resonance methods are used to draw these dependencies [A44].The obtained dependencies are important for the extraction of the equivalent dielectric parameters – equivalent dielectric

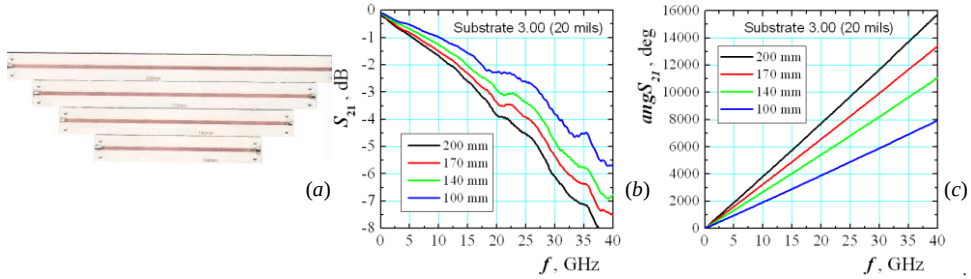

Fig. 3.6. Differential phase length (DPL) method: (*a*) four 50-Ohms microstrip lines with lengths 200, 170, 140 and 100 mm; Measured S_{21} dependencies (*b*) and phase delay (*c*)

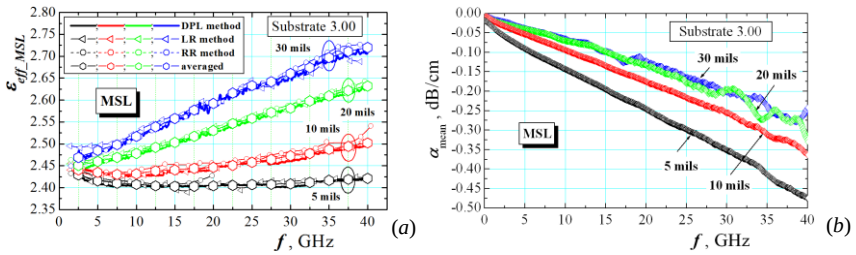

Fig. 3.7. Measured dependencies of ε_{eff_MSL} (*a*) and attenuation (*b*) by DPL and resonance methods for Substrate 3.0 with different thicknesses (in mils)

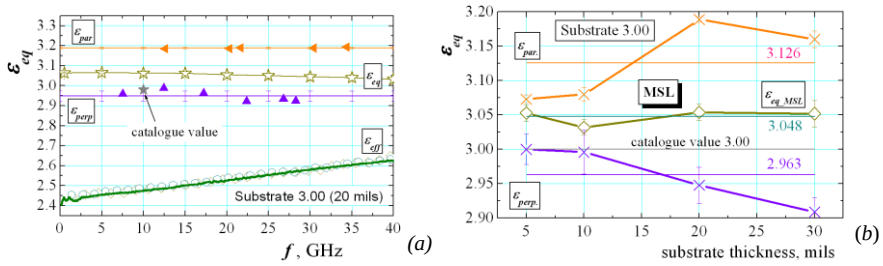

Fig. 3.8 *a*) Extracted dependencies of the equivalent dielectric constant ε_{eq_MSL} of MSL compared with measured parallel and perpendicular dielectric constants, ε_{par}, ε_{perp}; for Substrate 3.0 (20 m); *b*) parameters ε_{par} and ε_{perp}, compared with ε_{eq_MSL} for the same substrate versus the thickness

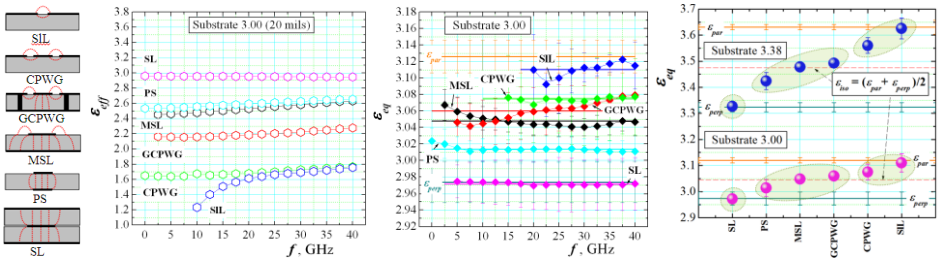

Fig. 3.9. Measured ε_{eff} (*a*) and extracted ε_{eq} (*b*) dependencies for six 50-Ohms planar transmission lines for Substrate 3.0 (20 mils); (c) averaged by the thickness and frequency ε_{eq} values of 6 planar lines for Substrate 3.0 and other Substrate 3.38. Legend: SL – stripline; PS – paired strips; MSL – microstrip lines; CPWG – coplanar waveguide; GCPWG – grounded CPWG; SlL – slot line.

constant ε_{eq} (in this case: MSL value ε_{eq_MSL}, shown in Fig. 3.8*a*) and the corresponding equivalent dielectric loss tangent $\tan\delta_{\varepsilon,eq}$. However, in the last case, the imperfect metallization influences the MSL attenuation in a big degree [37]; therefore, the conductor and radiation losses have to be taken into account for more accurate extraction of $\tan\delta_{\varepsilon,eq}$ [A43, A57] (details are presented in [2]).

For 10 years now, the equivalent dielectric constant ε_{eq} is an important parameter for the characterization of an anisotropic substrate of the different planar transmission lines. This parameter allows replacing the anisotropic substrate with an isotropic equivalent substrate in each RF design project, which is descri-bed with equivalent dielectric constant and equivalent dielectric loss tangent – see our concept in [A32, A44]. This is rather an effective approach and many substrate producers and 3D simulator developers started to share with the users the information for the equivalent dielectric constant, often called "design Dk" value. Fig. 3.8*b* presents a useful picture for Substrate 3.0 – comparison between the measured ε_{par}, ε_{perp} and ε_{eq_MSL} for different thickness. The results clearly show an important fact – the producers have managed to decrease the anisotropy for thin substrates, which are applicable in the mm-wavelength range.

The problem is that the equivalent dielectric constant depends on the type of the printed planar line on this substrate (see dependencies in Fig. 3.9*a*,*b*), i.e. from the concrete distribution of the parallel and perpendicular electric fields of

the dominant propagation mode in the given planar line. We managed to prove for the first time this fact in our work [A32] and then developed a special concept in [A44]. It turned out that this fact is a serious inconvenience for the application of the equivalent dielectric constant approach. However, we presented a solution based on the introduction of three groups of equivalent values – see the concept, presented in Fig. 3.9*c*. The proposal is users to use in their design pro-ject three different values of the equivalent dielectric constant ε_{eq} according to the designed planar structures: I – "stripline value" $\varepsilon_{eq\_SL} \sim \varepsilon_{perp}$ (or process, specification Dk, suitable for stripline and SIW); II – "microstrip value" $\varepsilon_{eq\_MSL} \sim (\varepsilon_{perp} + \varepsilon_{perp})/2$ (or design Dk, suitable for microstrip line, coupled MSL, paired strips, grounded coplanar waveguide and similar microstrip-like lines) and III – "coplanar value" $\varepsilon_{eq\_CPWG} \leq \varepsilon_{par}$ (or a new coplanar design Dk, suitable for slot-based planar lines: coplanar waveguide, slot and fin-line). The first two values are already in use as "process" and "design" values [38, 39] (our concept only explain the origin of these values), but the third value is new – it is suitable for coplanar and slot-line based structures. Many new publications confirm the usefulness of this our concept for reliable design of planar devices with equivalent dielectric constants (more details are given in [2]).

3.4. UTILIZATION OF 3D ELECTROMAGNETIC SIMULATORS AS AN AUXILIARY TOOL FOR MATERIAL CHARACTERIZATION BY RESONANCE MEASUREMENTS

The modern material characterization needs the utilization of powerful numerical tools for obtaining accurate results after modelling of very sophisticated measuring structures. Such software instruments could be the 3D EM simulators, which demonstrate serious capabilities in the modern RF design. Considering recent publications in the area of material characterization, it is easy to establish that the 3D simulators have been successfully applied for measurement purposes, too. The possibility to use commercial frequency-domain simulators as assistant tools for accurate measurement of the substrate anisotropy by the two-resonator method has been demonstrated for the first time in [A20]. Then, this option is developed for all types of considered resonators [A32], following few principles – simplicity, accuracy and fast simulations. Illustrative 3D models for the simplest structures, used in the two-resonator method (cylinder resonators R1 and R2), are drawn in Fig. 3.10*a*. Three main rules have been accepted to build these models for accurate and time-effective processing of the measured resonance parameters – 1) a stylized drawing of the resonators' body with equivalent diameters ($D_{eq1,2}$), actual height $H_{1,2}$ and equivalent wall conductivity $\sigma_{eq1,2}$; 2) an optimized number of line segments for construction of the curved cylindrical surfaces (line size less than 1/16 wavelength) and 3) a suitable for the operating mode splitting (1/4 or 1/8 from the whole resonator body; Fig. 3.10*b*), accompanied by appropriate boundary conditions at the cut-off planes. Although the real resonators have the necessary coupling elements and holes, the resonator bodies could be introduced into the model as pure closed cylinders and

this approach allows applying the eigenmode solver of the modern 3D simulators. The utilization of the eigenmode option for obtaining of the resonance frequency and the unloaded Q factor (notwithstanding that the modelled resonator is not fully realistic) considerably facilitates the anisotropy measurement procedure assisted by 3D simulators, if equivalent parameters have been additionally introduced and symmetrical resonator splitting has been done.

These optimized models increase the accuracy of the two-resonator methods for anisotropy measurements and allow us to evaluate the sensitivity of the corresponding resonators (with the used TE or TM modes) to the actual sample anisotropy – see dependencies in Fig. 3.11. The analysis of the obtained results shows that the chosen modes in the different pairs of measurement resonators have very good selectivity to the corresponding dielectric constant of the sample in the resonator along a given direction with errors less than ±0.25 % for the nor-malized resonance frequency f_{aniso}/f_{iso} and less than ±0.5 % for the normalized Q factor Q_{aniso}/Q_{iso}, when the anisotropy varies in the intervals ΔA_{ε}, $\Delta A_{\tan\delta\varepsilon} = \pm 10$ % even for relatively thick samples (excepting for SCR).

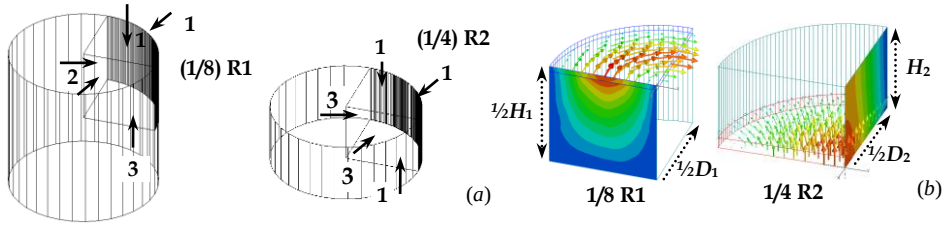

Fig. 3.10. (*a*) Equivalent 3D models of a pair of two cylinder resonators R1/R2 and boundary conditions (legend: 1 – finite conductivity (σ_{eq}); 2 – E-field symmetry; 3 – H-field symmetry); (*b*) Simulated E-field scalar and vector distribution in the measurement resonators (1/8 R1 and 1/4 R2)

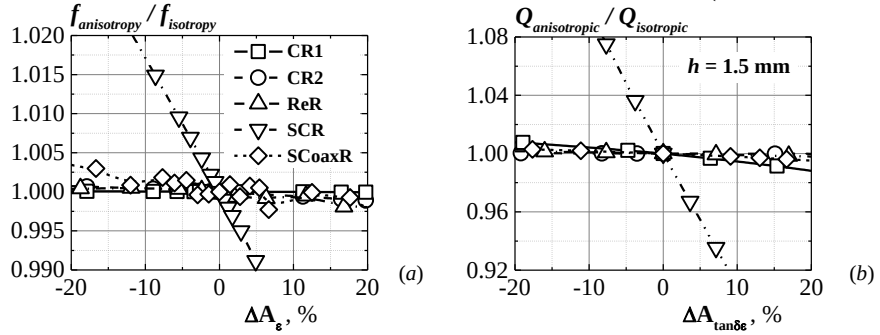

Fig. 3.11. Dependencies of the normalized resonance frequency (*a*) and Q-factors (*b*) of the used resonance modes for anisotropic and isotropic samples versus dielectric anisotropy ΔA_{ε} , $\Delta A_{\tan\delta\varepsilon}$

3.5 PROBLEMS WITH RELIABLE 3D SIMULATIONS OF MICROSTRIP LINES ON ANISOTROPIC SUBSTRATES

The microwave engineers have two possibilities to take into account the material anisotropy in their numerical design projects – to replace the real aniso-

tropic structure with isotropic equivalent, described by the equivalent dielectric constant ε_{eq}, or to use the "anisotropic material" option of the modern 3D simulators, introducing the pair of values ε_{par} and ε_{perp}. The concept and design accuracy applying the first option is already described above. There exist only a few papers, where the second option has been directly applied, but with not so expressed benefits (see references in [A49]).

Let's compare both options. Several 3D models have been constructed for six popular planar transmission lines on an anisotropic substrate, following the accepted in the RF design standard principles for ports, radiations boxes, etc. (see Fig. 3.12*a* for MSL). We selected one typical Substrate 3.38 with a middle anisotropy, measured by the two-resonator method in the range 5-40 GHz: ε_{par} = 3.66; ε_{perp} = 3.345. The corresponding equivalent dielectric constant is ε_{eq} = 3.48, measured by the DPL method. Fig. 3.12*b* presents the simulated frequency ε_{eff} - dependencies of 50-Ohms MSL in two options of the used 3D simulator: 1) isotropic equivalent substrate with $\varepsilon_{xx} = \varepsilon_{yy} = \varepsilon_{zz} = \varepsilon_{eq}$ and 2) real anisotropic substrate with $\varepsilon_{xx} = \varepsilon_{yy} = \varepsilon_{par}$; $\varepsilon_{zz} = \varepsilon_{perp}$. The ε_{eff} values calculated by the second (ani-

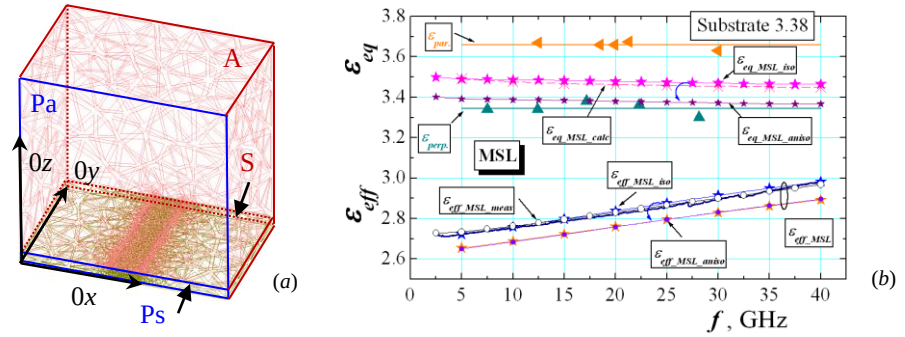

Fig. 3.12 *a*) 3D model of MSL on an anisotropic substrate with selected two rectangular volumes S (substrate) and A (air above) and two *x*0*z* planes Ps and Pa at the input port; *b*) Comparison between simulated frequency dependencies of the effective ε_{eff} and the corresponding equivalent ε_{eq} dielectric constants of MSL on an anisotropic substrate using options isotropic/anisotropic material

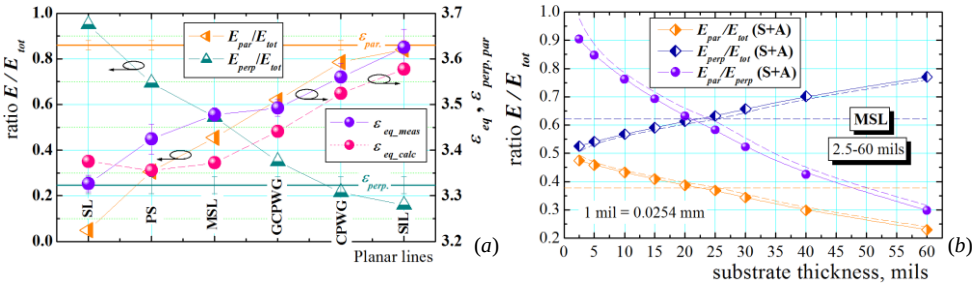

Fig. 3.13 *a*) Measured and calculated ε_{eq} values by simulated phase delay in several planar transmission lines and simulated normalized parallel and perpendicular E fields in these lines; *b*) Distribution of normalized parallel and perpendicular electric fields in the united box volumes S+A (substrate and air box above) of 50-Ohms MSL (dashed curves – for united Ps + Pa planes on the radiation box wall – Fig. 3.12*a*)

sotropic) option are visibly smaller, than the values for the isotropic case (the re-calculated equivalent dielectric constant is 3.38 instead 3.48 for MSL, i.e. 2.8-% decrease). Fig. 3.13*a* presents these differences for other investigated planar lines: from 0.5 up to 3 % decrease, which is not acceptable for a reliable RF design. In fact, the biggest differences appear for MSL and MSL-like lines, e.g. for coupled MSL (up to 4 % decrease, not shown). In the same time the course of the curves, representing the distribution of the normalized parallel and perpendicular electric fields, E_{par}/E_{tot} and E_{perp}/E_{tot}, in the whole structures fully correspond to the position of the measured ε_{eq} values between ε_{par} and ε_{perp} values of each given planar line. Therefore, we can try to bind the ε_{eq} values directly to the field distribution. In [A48] we proposed a more accurate, field model for calculation of the ε_{eq} values. For this purpose, we include in the MSL model (Fig. 3.12*a*) several new artificial volume and plane objects, where we can easily calculate the integrated complex E fields by the incorporated "field calculator" in the simulators. The aim is to determine both field ratios E_{par}/E_{tot} and E_{perp}/E_{tot} in these volumes or planes and to calculate ε_{eq_MSL} by the expression

$$\varepsilon_{eq_{MSL}} \cong \left(\left.\frac{E_{par}}{E_{tot}}\right|_{MSL} \times \varepsilon_{par}\Big|_{sub} + \left.\frac{E_{perp}}{E_{tot}}\right|_{MSL} \times \varepsilon_{perp}\Big|_{sub} \right), \tag{8.3}$$

The obtained results are quite informative. The calculated ratio for substrate only is E_{par}/E_{perp} = 0.19/0.81 in the volume S. If we determine ε_{eq_MSL} by (1) applying these ratios, the obtained dependencies are very close to the $\varepsilon_{eq\_sim\_phase}$ dependencies, obtained by the simulated phase delay (i.e. by the MSL S parameters) – see Fig. 3.12*b*. But if we now apply the E-field ratios in the whole structure, i. e. $E_{par}/\ E_{perp}$ = 0.39/0.61 in the united volumes S+A, the calculated ε_{eq} values are very close to the measured values ε_{eq_meas} (or to the values, obtained by the simulator for option "equivalent isotropic substrate"). This fact is very optimistic. It points the direct connection between the calculated actual ratio E_{par}/E_{perp} for each planar structure (MSL in the considered case) and the measured equivalent dielectric constant.

The obtained positive results for the possibility to predict the actual values of the equivalent dielectric constant only on the base of the calculated near-field distribution of the parallel and perpendicular electric fields in MSL allow us to propose a reliable method for a direct determination of this important parameter without to perform any specialized time-consuming measurements. But to implement this method, we have to investigate the influence of the MSL parameters over the field distribution. Fig. 3.13*b* presents the most important dependences E_{par}/E_{tot} and E_{perp}/E_{tot} on the substrate thickness, which can be used directly in expression (1). According to the expectations, the parallel component of the electric field plays a bigger role for thinner substrates and v.v. Therefore, we can average the dependencies and write an approximate expression, which

$$\varepsilon_{eq\,MSL} \cong \left((0.38 \pm 0.02) \times \varepsilon_{par}\Big|_{sub} + (0.62 \pm 0.02) \times \varepsilon_{perp}\Big|_{sub}\right), \quad (8.4)$$

ensures the best accuracy for substrates with thickness 20-30 mils. The other MSL and substrate parameters (e.g. metallization thickness, absolute dielectric constant, losses) don't play so important role. Now, if we calculate values $\varepsilon_{eq\_MSL\_calc}$ by (8.4), they practically coincide with the measured ones $\varepsilon_{eq\_MSL\_iso}$ in the presented case in Fig. 3.12*b* (more results are given in [2]).

4. CONCLUSIONS

In this paper, we summarize the main results from our 18-year research work devoted to the characterization of the dielectric properties of materials used in modern microwave electronics. First of all, we prove the assumption that the well-determined complex dielectric and magnetic constants of the materials are important not only for improving the accuracy of the modern 3D design of nowadays electro-dynamic structures but also because the integral character of these parameters ensures valuable information for the real material composition, structure, character of inclusions, building blocks and unit cells orientation, used technology, conditions for the material preparation, etc. We have shown that additional very useful information can be achieved when the actual anisotropy of the material constants has been determined and compared – different behaviour of their permittivity/permeability in different directions. Our numerical models and experimental methods for characterization of the sample dielectric and magnetic properties including their anisotropy give satisfactory accuracy practically for all possible applications. The full set of the implemented resonance and broadband measurement methods in our Microwave laboratory gives us the possibility for deep investigation and characterization of a variety of different materials in the nowadays electronics – microwave substrates, ceramics, multilayer composites, different dielectric mixtures, 3D printed dielectrics, textile fabrics, metamaterials, thin micro- and nano-films, carbon-content materials, fresh and dry plant tissues, etc. More information for the concrete properties and peculiarities and especially for the artificial anisotropy of these materials has been given in the second part of this survey [2].

Acknowledgements. The investigations have been supported by the Bulgarian National Scientific Fund under Contract No. DN-07/15/2018-19.

REFERENCES

[1] P. I. Dankov (2018), *Asia-Pacific Microwave Conference*, Nov. 6-9, 2018, Kyoto, Japan, University Poster Exhibition, Nov. 2018, DOI: 10.13140/RG.2.2.12158.02881

[2] P. I. Dankov (2019), *Annuaire de l'Université de Sofia "St. Kliment Ohridski", Faculté de Physique*, v. 112 (this issue; part 2)

[3] Y. Xu, Y. Fu, and H. Chen (2017), *Optics Express*, vol. 25, no. 5, 6 March 2017, pp. 4952-4966, https://doi.org/10.1364/OE.25.004952

[4] G. Singh, Rajni, A. Marwaha (2015), Int. *Journal of Engineering Trends and Technology* (*IJETT*), vol. 19, no. 6, Jan 2015, pp. 305-310, ISSN: 2231-5381, http://www.ijettjournal.org

[5] Pioneering 21st Century Electromagnetics and Photonics Laboratory, University of Texas at El Paso, College of Engineering, http://emlab.utep.edu/research.htm
[6] K. S. Cole, R. H. Cole (1941), *J. Chem. Phys.*, 9, 1941, pp. 341-351
[7] European Commission (Directorate-General for Research, Communication Unit) (2010), "Nano-structured Metamaterials", Editor in Chief Anne F. de Baas, B-1049 Brussels, online
[8] R. C. Rumpf (2015), *Solid State Physics*, vol. 66, pp. 213-300
[9] A. Sihvola (1999), "Electromagnetic Mixing Formulas and Applications", The Institute of Electrical Engineers, *Electromagnetic Waves Series 47*, London, UK
[10] G. G. Raju (2017), "Dielectrics in Electric Fields, Ch. 2, *CRC Press, Taylor & Francis Group*
[11] A. D. Boardman, and K. Marinov (2006), *Phys. Rev. B*, vol. 73, no.16, pp. 165110-1/7
[12] P. Gay-Balmaz, O. J. F. Martin (2002), *Journal of Applied Physics*, v. 92, n. 5, pp. 2929-2936
[13] A. Armghan, X. Hu, and M. Y. Javed (2018), *IGI Global*, DOI: 10.4018/978-1-5225-4180-6
[14] C. R. Garcia, J. Correa, D. Espalin, J. H. Barton, R. C. Rumpf, R. Wicker, and V. Gonzalez (2012), *PIERS Letters*, vol. 34, pp. 75-82
[15] W.X. Jiang, J.Y. Chin and T. J. Cui (2009), *Materials Today*, vol. 12, No. 12, pp. 26-33
[16] Handbook of Magnetic Materials (2015), Vol. 24, Ed. by K.H.J. Buschow, Ch. 3 "Advances in Magnetoelectric Materials and Their Application", http://dx.doi.org/10.1016/bs.hmm.2015.10.001
[17] IPC TM-650 2.5.5.5 (1998) Test Methods Manual, http://www.ipc.org/html/fsstandards.htm
[18] National Institute of Standards and Technology (NIST), USA, https://www.nist.gov/mml/orm
[19] National Measurement Institute, NPL, UK, Electromagnetic measurements on materials, https://www.npl.co.uk/products-services/electromagnetic-materials/
[20] L. F. Chen, C. K. Ong, C. P. Neo, V. V. Varadan, V. K. Varadan (2004), "Microwave Electronics: Measurement and Material Characterization", John Wiley &Sons, Ltd., Ch. 7
[21] J. Krupka (2006), *Meas. Sci. Technol.*, 17, R55–R70, doi:10.1088/0957-0233/17/6/R01
[22] A. Gaebler, F. Goelden, S. Mueller, R. Jakoby (2008), *Proc. 38th EuMC*, Oct, 2008, Amsterdam, The Netherlands, pp. 909-912
[23] W. E. Courtney (1970), " *IEEE Trans. on MTT*, v. 18, no. 8, pp. 476-485
[24] G. Kent (1988), *IEEE Trans. on MTT*, vol. 36, no. 10, pp. 1451–1454
[25] M. D. Janezic and J. Baker-Jarvis, *IEEE Trans. on MTT*, vol. 47, no. 10, pp. 2014–2020
[26] J. Krupka, R.N. Clarke, O.C. Rochard, A.P. Gregory (2000), *Proc. 13th MIKON-2000*, Wroclaw, Poland; DOI: 10.1109/MIKON.2000.913930
[27] X. Zhao, C. Liu, and L. C. Shen (1992), *IEEE Trans. on MTT*, vol. 40, no. 10, pp. 1951–1958
[28] J. Baker-Jarvis and B. F. Riddle (1996), *NIST, Boulder*, CO, Tech. Note 1384, Nov. 1996
[29] J. Krupka, D. Cros, M. Aubourg, and P. Giullion, *IEEE Trans.on MTT*, vol.42, no.1, pp.56-61
[30] G. Mumcu, K. Sertel, and J. L. Volakis (2008), *IEEE Trans.on MTT*, vol.56, no.1, pp.217-223
[31] A. B. Bereskin, US Patent 50083088, Jan. 1992
[32] J. C. Rautio, R. L. Carlson, B. J. Rautio, S. Arvas, *IEEE Ttans on MTT*, vol. 59, no. 3, pp. 748-754
[33] X.-C. Zhu, W. Hong, K. Wu, H.-X. Zhou, *Proc.APMC'2012*, Kaohsiung, Taiwan, pp.860-862
[34] H. Kawabata, K. Hasuike, Y. Kobayashi, Z. Ma (2006), *Proc. of 36th EuMC*, Manchester, UK,
[35] Y. Kato, M. Horibe (2019), IEEE Trans on Instrumentation and Measurement (under publication)
[36] R. Sturdivant (2014), "Microwave and Millimeter-Wave Electronic Packaging", Artech House, ISBN 978-1-60807-697-0, 2014, Ch. 2
[37] A.F. Horn III, P.A. LaFrance, J.W. Reynolds, and J. Coonrod (2012), *Circuit World*, 38, no.4, pp. 219-231
[38] J. Coonrod (2011), *Microwave Journal*, vol. 54, No. 5, May 2011, pp. 132-144
[39] J. Coonrod and A. F. Horn III (2011), *High Frequency Design*, July 2011

AUTHORS' REFERENCES

[A1] I. P. Ghanashev, S. A. Ivanov, P. I. Dankov and J. Kutzarova (1988), *Proc. 8th MIKON*, Gdansk, Poland, April 1988, pp. 122-126
[A2] P. I. Dankov, S. A. Ivanov and I. P. Ghanashev (1989), *Proc. 6th Int. School on Microwave Physics and Technique*, Varna, Bulgaria, Sept. 1989, pp. 733-738
[A3] S. A. Ivanov and P. I. Dankov (1995), *Proc. ISRAMIT'95*, Kiev, Ukraine, pp. 574-577
[A4] P. I. Dankov (1996), *Proc. 13th Int. Conf. on Microwave Ferrites*, Romania, pp. 21-27
[A5] P. I. Dankov, S. A. Ivanov (1997), *Annuaire de l'Université de Sofia "St. Kliment Ohridski", Faculté de physique*, 91, 1997, pp. 5-31
[A6] S. A. Ivanov and P. I. Dankov (1998), *Proc. 7th Int. Conf. on Mathematical Methods on Electromagnetic Theory*, Kharkov, Ukraine, pp. 378-380
[A7] P. I. Dankov (1998), *Proc. 14th Int. Conf. on Microwave Ferrites*, Hungary, pp. 166-170
[A8] S.A. Ivanov, P.I. Dankov (2000), *2nd International Symposium of Trans Black Sea Region Applied Electromagnetism*, DOI: 10.1109/AEM.2000.943254

[A9a] P. I. Dankov, I. T. Vineshki (2000), *Journal of Balkan Phys. Letters*, Proc. 4th General Conf. of BPU
[A9] V. Peshlov, I. Slavkov, and P. Dankov (2001), *Proc. EuMC'2001*, vol. 3, London, UK, pp. 257-260
[A10] M. Gatchev, S. Kamenopolsky, V. Boyanov, P. Dankov (2002), *14th MIKON'2002*, Gdansk, Poland, pp. 189-192
[A11] J. Bozmarov, R. Traykov, V. Peshlov, P. Dankov (2002), *14th MIKON'2002*, Gdansk, Poland, DOI: 10.1109/MIKON.2002.1017986
[A12] S.A. Ivanov and P.I. Dankov (2002), *J. Electrical Engineering*, vol. 53, No. 9s, pp. 93–96
[A13] P. Dankov, S. Kamenopolsky, V. Boyanov (2003), *14thMicrocoll'2003*, Budapest, Hungary, pp.217-220
[A14] P. I. Dankov (2004), *15th MIKON'2004*, Warsaw, Poland, May 2004, vol. 1, pp. 151-154
[A15] V. Peshlov, S. Alexandrov and P. Dankov (2004), *15th MIKON'2004*, Warsaw, Poland, v. 2, pp. 562-566
[A16] P.I. Dankov, S.M. Kolev, S.A. Ivanov (2004), *17th EMFM-2004*, Warsaw, Poland, pp. 89-93
[A17] I. Nedkov, S. Kolev, P. Dankov, S. Alexandrov (2004), *Proc. IEEE Int. Spring Seminar on Electronics Technology 27th ISSE 2004*, Sofia, Bulgaria, pp. 577-579
[A18] P. I. Dankov, and S. A. Ivanov (2004), *34th EuMC'2004*, Amsterdam, Holland, pp. 753-756
[A19] P. I. Dankov, V. P. Levcheva, and V. N. Peshlov (2005), *35th EuMC'2005*, Paris, France, pp. 515-519
[A20] V. N. Peshlov, P. I. Dankov, B. Hadjistamov (2005), *1st European Conference on Antennas and Propagation EuCAP'2005*, France, Nice, No. 349840PD (available IEEE Xplore)
[A21] P. I. Dankov, B. Hadjistamov, and V. P. Levcheva (2006), *Proc. IVth Mediterranean Microwave Symposium (MMS'2006)*, Genoa, Italy, Sept. 19-21, 2006 (available IEEE X-plore)
[A22] P. I. Dankov (2006), *IEEE Trans.on MTT*, vo. 54, no.4, pp. 1534-1544
[A23] B. N. Hadjistamov, V. P. Levcheva, and P. I. Dankov (2007), *Proc. Vth Mediterranean Microwave Symposium (MMS'2007)*, Budapest, Hungary, pp. 183-186
[A24] P. I. Dankov, V. P. Levcheva, and I. I. Arestova (2007), *Proc.ICMF'2007*, Budapest, Hungary, pp.27-30
[A25] P. I. Dankov and B. Hadjistamov (2007), *37th EuMC'2007*, Munich, Germany, pp. 933-936
[A26] P. I. Dankov, V. N. Peshlov, M. Gachev (2008), *30th ESA Antenna Workshop on Antennas for Earth Observation, Science, Telecommunications and Navigation Space Missions*, Nordwijk, The Netherlands, pp. 505-508 (invited COST paper)
[A27] V. P. Levcheva, B. N. Hadjistamov. P. I. Dankov (2008), *Bulg. J. Phys*., 35, pp. 33-52
[A28] P. Dankov, P. Stefanov, V. Gueorguiev, T. Ivanov (2008), *J. of Physics*, Conf. Series, pp. 202-209
[A29] V. P. Levcheva, I. I. Arestova, B. R. Nikolov, and P. I. Dankov (2009), *Telfor Journal*, Vol. 1, No. 2, 2009, pp. 57-60
[A30] S. R. Baev, B. N. Hadjistamov, and P. I. Dankov (2009), "Lüneburg Lenses as Communication Antennas", *Annuaire de l'Universite de Sofia "St. Kliment Ohridski", Faculte de Physique*, 102, 2009, pp. 67-84
[A31] P. Dankov, B. N. Hadjistamov, I. Arestova, V. Levcheva (2009), *PIERS online*, vol. 5, no. 6, pp.501-505
[A32] P. I. Dankov (2010), "Dielectric Anisotropy of Modern Microwave Substrates", *Chapter 4 in "Microwave and Millimeter Wave Technologies from Photonic Bandgap Devices to Antenna and Applications"*, ed. by Igor Minin, In-Tech Publ., Austria, Jan. 2010, ISBN 978-953-7619-66-4
[A33] P. I. Dankov, M. I. Kondeva, and S. R. Baev (2010), ISBN: 978-1-4244-4883-8, *iWAT Conference*, Lisbon, Portugal, DOI 10.1109/IWAT.2010.5464930 (online IEEE Xplore)
[A34] K. Zlatkov, P. Dankov (2011), *Microwave Review*, ISSN 14505835, UDK 621.3.049.77, pp. 29-35
[A35] B. N. Hadjistamov, P. I. Dankov (2011), *Bulg. J. Phys.* 38, pp. 191–198
[A36] P. Dankov, Z. Kiss'ovski (2012), *XXI ESCAMPIG*, Viana do Castelo, Portugal
[A37] P. I. Dankov (2013), *2nd National Congress on Physical Sciences*, Sofia, Bulgaria (online)
[A38] P. I. Dankov (2014), *J. of Physics: Conf. Series 516*, DOI:10.1088/1742-6596/516/1/012001
[A39] R. B. Borisov, K. I. Zlatkov, and P. I. Dankov (2014), E+E Journal, vol. 49, No. 3-4, 2014, pp. 7-12
[A40] M. Gachev, V. Boyanov, S. Kamenopolsky, V. Peshlov, B. Marinov, and P. Dankov (2014), DOI: 10.1109/EuCAP.2014.6902312, *8th EuCAP'2014*, The Hague, The Netherlands, (online)
[A41] M. Gachev, P. Dankov (2015), *8th Management Committee Meeting and Workshop*, Sofia, Bulgaria
[A42] P. Dankov, V. Peshlov, and and T. Amla (2015), *8th Management Committee Meeting and Workshop*, Sofia, Bulgaria, Sofia University, Aula Magna, (online available)
[A43] P. Dankov, S. Kamenopolski, V. Peshlov, R. Traykov (2016), *9th GSMM2016 7th ESA Workshop on Millimetre-Wave Technology and Applications*, Espoo, Finland (IEEE Xplore)
[A44] P. I. Dankov (2016), *EuMC'2016*, London, UK, pp. 158-161
[A45] M. Gachev, and P. Dankov (2016), NSS-07-0601, *7th Nano–Satellite Symposium and 4th Unisec-Global Meeting*, Kamchia, Bulgaria, 2016 (online available)
[A46] P. I. Dankov (2017), *iWAT'2017*, Athens, Greece, pp.61-64 (IEEE Xplore)
[A47] P. I. Dankov (2017), *FERMAT*, Vol. 22, Communication 9, ISSN 2470-4202 (see [A46])
[A48] P. I. Dankov (2017), Proc. *IEEE MTT-S Int. Conf. NEMO'2017*, DOI: 10.1109/NEMO.2017.7964199
[A49] P. I. Dankov (2017), *Proc. IEEE MTT-S Int. Microwave Workshop Series on Advanced Materials and*

Processes, Pavia, Italy, (IEEE Xplore)
[A50] P. I. Dankov (2017), *Proc. 47th EuMC'2017*, Nurenburg, Germany, pp. 954-957 (online)
[A51] P. I. Dankov, M. I. Tsatsova, and V. P. Levcheva (2017), *Proc. of PIERS'2017*, Singapore
[A52] P. I. Dankov, and I. I. Iliev (2017), *Proc. of PIERS'2017*, Singapore
[A53] P. I. Dankov (2018), *8th Int. Workshop and Summer School on Plasma Physics (IWSSPP'2018*), Kiten, Bulgaria, (invited paper; online); Journal of Physics: Conf. Series, IOP Publishing, 2019
[A54] P. I. Dankov (2018), *Proc. 48th EuMC*, Madrid, Spain, (IEEE Xplore)
[A55] V. Levcheva, P. Dankov (2018), *Bulg. J. Phys.*, v. 45, pp. 264–274
[A56] P. Dankov, V. Levcheva, M. Iliev (2018), Proc. *Metamaterials'2018*, Espoo, Finland, online
[A57] P. Dankov, R. Traykov, V. Peshlov, and S. Kamenopolski (2018), *Asia-Pacific Microwave Conference APMC2018*, Kyoto, Japan, (IEEE Xplore)
[A58] P. I. Dankov, M. T. Iliev, V. P. Levcheva (2018), *Bulgarian Chemical Communications*, Vol. 50 (Special Issue F), pp. 126-134
[A59] M. Gachev, and P. Dankov (2019), „Microwaves in Bulgaria", *1st European Microwave Conference in Central Europe*, Prague , Czech Republic, IEEE Xplore (online)
[A60] P. Dankov; B. Tzaneva; V. Videkov (2019), SPIE Conference Proceeding, Proceedings Volume 11332, International Conference on Quantum, Nonlinear, and Nanophotonics 2019 (ICQNN 2019) (online)
[A61] P. I. Dankov (2019), *IEEE 19th Mediterranean Microwave Symposium*, Tunisia, Nov.2019 IEEE Xplore
[A62] P. Dankov, S. Kolev, T. Koutzarova (2019), VIET2019, Sept. 2019, Sozopol, Bulgaria (to be published in Journal of Physics: Conf. Series, IOP Publishing, 2020)
[A63] P. Dankov, V. Levcheva, S. Kolev, and T. Koutzarova (2019), VIET2019, Sept. 2019, Sozopol, Bulgaria (to be published in Journal of Physics: Conf. Series, IOP Publishing, 2020)
[A64] P. Dankov, V. Levcheva, P. Sharma (2020), iWAT2020, Feb. 2020, Bucharest, Romania (online available: IEEE Xplore)
[A65] P. Dankov (2020), "Anisotropy of artificial materials and how to characterize it?" - COST Action CA18223 SyMat Meeting – Prague, Feb. 2020 (online)
[A66] P. Dankov (2020), "Material Characterization in the Microwave Range – another look to the properties of modern artificial dielectrics", (invited lecture; 10th International Advances in Applied Physics & Materials Science Congress & Exhibition (APMAS2020), October 14-20, 2020, Oludeniz, Turkey (to be published in ACTA Materialia Turcica)
[A67] V. Levcheva, and P. Dankov (2020), "Characterization of Microwave Absorbers, Including Multilayer Nanoabsorbers", 22nd International Conference Materials, Methods & Technologies, 29 Aug. – 1 Sept. 2020, Burgas, Bulgaria (to be published in Materials, Methods & Technologies; ISSN 1314-7269)
[A68] P. Dankov, and V. Levcheva (2020), "Investigations of Artificial Metamaterials and Multilayer Nano-Composites in External Magnetic Field", 22nd International Conference Materials, Methods & Technologies, 29 Aug. – 1 Sept. 2020, Burgas, Bulgaria (to be published in Materials, Methods & Technologies; ISSN 1314-7269)